Non-equilibrium steady state in the Mott insulator Ca_2RuO_4

Ichiro Terasaki[1], Isuzu Sano[1], Kosuke Toda[1], Shuji Kawasaki[1], Akitoshi Nakano[1], Hiroki Taniguchi[1], Hai Jun Cho[2], Hiromichi Ohta[2] and Fumihiko Nakamura[3]

[1]*Department of Physics, Nagoya University, Nagoya 464-8602, Japan*
[2] *Research Institute for Electronic Science, Hokkaido University, Sapporo 001-0020, Japan*
[3] *Department of Education and Creation Engineering, Kurume Institute of Technology, Kurume 830-0052, Japan*

We have measured and analyzed the nonlinear conduction of the Mott insulator Ca_2RuO_4 with square wave and square-pulse currents around room temperature with an infrared camera as a contactless thermometer. By combining the thermal diffusivity measurements, we have found that the temperature increase due to self heating is explained by the conduction of the Joule heat through the sample to the heat bath. We further find a time scale of the nonlinear conduction to be 20 ms, which is consistent with thermal relaxation time of the sample. We propose that a steady dissipation of external energy flow characterizes the non-equlibrium steady state of Ca_2RuO_4, rather than a steady current flow.

Statistical physics has described various properties of macroscopic objects in thermal equilibrium by taking statistical average of observable for a given microscopic Hamiltonian, and thereby bridged the gap between microscopic and macroscopic scales. As a next step, great efforts have been long devoted to extend its applicable range towards non-equilibrium states. For this purpose, a good playground will be non-equilibrium steady states (NESS), where energy and particle flow steadily. The presence of flow clearly defines such states to be out of thermal equilibrium, but except for this, all the macroscopic variables are expected to be independent of time in which thermodynamics may partially remain valid.[1,2] NESS is seen everywhere in nature: water flow in a river, chemical reaction with exchange of energy, and metabolism in biological systems.[3]

An electrical conductor subject to an external constant current offers a prime example of NESS, in which there exist electrical current flow of I (particle flow), energy flow IV from the current source, and Joule heat Q to the heat bath.[4] Although most of ohmic conductors are not interesting as NESS, here are some exceptional conductors; a charge density material shows macroscopic deformation against current,[5] and a toroidal-moment-ordered material shows current-induced magnetization.[6] These examples clearly indicate that thermodynamic variables such as volume and magnetization can vary with non-thermodynamic dissipative parameter of I.

The Mott insulator Ca_2RuO_4 occupies a unique position in strongly correlated electron systems in the sense that small external impetuses can change the ground state. This oxide crystallizes in the K_2NiF_4 type structure, where the conductive RuO_2 planes consisting of the corner-shared RuO_6 octahedra are stacked with the CaO double layer along the c axis. Nakatsuji et al.[7] first synthesized this oxide, and later Alexander et al.[8] found a first-order metal-insulator transition around 360 K. Braden et al.[9] performed detailed structure analysis using neutron scattering, and found that the transition accompanied substantial changes in the distortion and rotation of the Ru-O octahedra, which implies a strong electron-lattice coupling. Nakamura et al.[10] discovered itinerant ferromagnetism below 30 K under a relatively low pressure of 3 GPa, and discovered superconductivity above 10 GPa below 0.6 K.[11] This again shows the strong electron-lattice coupling, in which external pressure squeezes the lattice to change the electronic ground state.

We have studied the nonlinear conduction in Ca_2RuO_4,[12–16] since Nakamura et al.[17] discovered a giant nonlinear conduction at room temperature. Okazaki et al.[12] established a measurement technique of nonlinear conduction using infrared thermometer, and successfully separated the intrinsic nonlinear conduction from self heating. Nishina et al.[14] observed the Seebeck coefficient enhanced by a constant current flow. Tanabe et al.[15] observed a large negative capacitance under constant dc bias, and explained this in terms of transient resistive response due to nonlinear conduction. Very recently, Okazaki et al.[16] found that the lattice constants change with current; this phenomenon is understood in terms of the current-induced Mott gap suppression. As mentioned above, I, IV and Q are present in NESS, but it is to be explored which characterizes NESS in Ca_2RuO_4. To see this we report the square-wave response and the square pulse response in the electrical conduction of Ca_2RuO_4. The former response corresponds to an ac flow of I with steady flows of IV and Q, whereas the latter corresponds to time-dependent response of I, IV and Q. By comparing the two experiments, we address what characterizes NESS in this particular oxide.

Single-crystal samples of Ca_2RuO_4 were grown by a floating-zone method. The detailed conditions and characterization were given elsewhere.[18] In-plane thermal diffusivity was measured with a home-made measurement station based on an ac calorimetric method.[19] The details will be published in a separate paper. Cross-plane thermal diffusivity was measured at room temperature by the time domain thermoreflectance (PicoTR, PicoTherm Co.)[20] The 100-nm-thick Mo was deposited on the sample as a transducer by dc sputtering. The results were simulated using the packaged software. Using a bulk density ρ of 4.5×10^3 kg/m^3 and a specific heat c of 6.9×10^2 J/kgK,[21] the in-plane and cross-plane thermal conductivity κ was evaluated to be 5.1 and 1.8 W/mK at room temperature, respectively, from the measured thermal diffusivity within an uncertainty of ±20%.

Figure 1 (a) shows a photographic image of a sample with

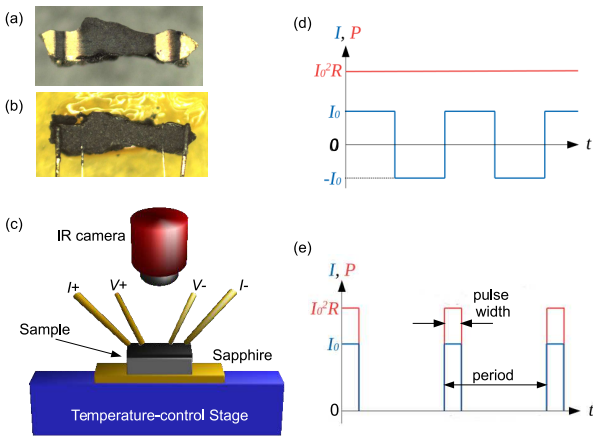

Fig. 1. (Color online) (a) A single-crystal sample of Ca_2RuO_4 used in the present experiment. Gold films are sputtered to ensure good electrical contact for the four-probe configuration. (b) The same sample as in (a) on top of which four gold wires are attached. The whole surface was pained by black paint. (c) Schematic for the experimental setting. (d) Response for square wave current. Note that the input power P is independent of time. (e) Response for square pulse current.

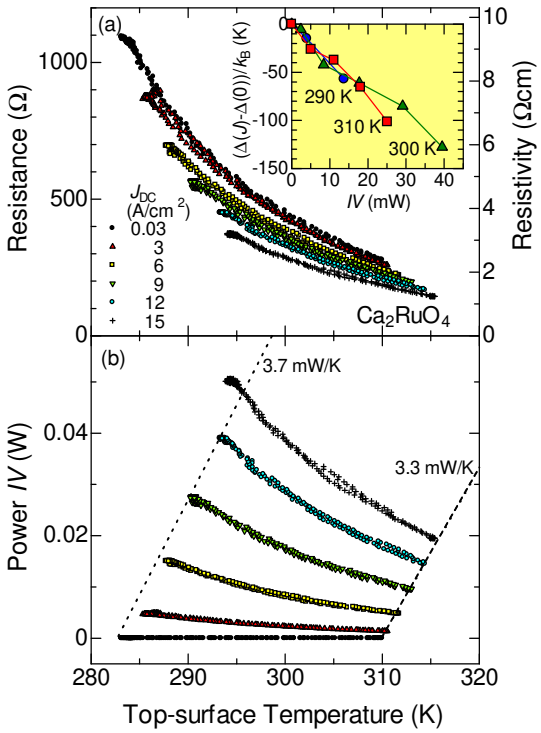

Fig. 2. (Color online) (a) Nonlinear resistance and resistivity of Ca_2RuO_4 plotted as a function of the temperature at the top surface of the sample (top-surface temperature) against various external current densities. The current is applied along the in-plane direction. (b) Supplied energy flow from the current source plotted as a function of top-surface temperature against various external current densities. The dotted and dashed lines represent an estimation of cross-plane heat flow to the bath (see text). The inset shows suppression of the Mott gap evaluated from the nonlinear resistivity (see text).

a dimension of 1.57×0.30×0.26 mm^3 used in the nonlinear conduction experiment. The four stripe lines of Au film were sputtered on the sample surface of the c plane to ensure low contact resistance. Au wires were then attached with silver paint on the Au stripes, and the whole surface was covered with black paint to ensure 100% radiation efficiency, as shown in Fig. 1(b).

The experimental setup is schematically shown in Fig. 1(c). The sample was glued on a sapphire plate with apiezon grease, and the sapphire plate was firmly attached on a temperature-control bath (As-One, CS-20). The temperature of the bath was swept from 253 to 313 K with a rate of 6 K/min. The top-surface temperature (the temperature between the voltage pads at the top surface of the sample) was monitored with an infrared thermal image camera with a spatial resolution of 0.15×0.15 mm^2 (Nihon Avionics, InfRec R300). The nonlinear conduction was measured using a four-probe method with a nano-voltmeter (Keithley 2182) synchronized by a DC/AC current source (Keithley 6221). In addition to conventional dc measurement, two ac sequences were employed. As shown in Fig. 1(d), the one sequence was to use square wave current, where the electrical current flow was alternating, with a steady energy flow. The frequency varied from 10^{-1} to 10^4 Hz. The signal was collected by the synchronized nano-voltmeter below 10 kHz, and was obtained with the ac mode of a multimeter (Agilent 34401A) at 10 kHz. The other sequence was to use square-pulse current as shown in Fig. 1(e), where a square short pulse was followed by a zero current, and repeated with a period of 83 ms. The pulse width was varied from 1 to 12 ms.

Figure 2(a) shows the resistance and resistivity of the single-crystal sample of Ca_2RuO_4 along the in-plane direction plotted as a function of top-surface temperature. With increasing external current density, the resistivity concomitantly decreases at all the temperatures, exhibiting nonlinear conduction. Following the method established by Okazaki et al.,[12] we use the temperature obtained from infrared camera as the horizontal axis, where the temperature increase due to self-heating is already taken into account. Actually, for higher current densities, the measured range of the top-surface temperature shifts to higher temperatures. Comparing the resistivity at the same top-surface temperature, we find that it decreases with increasing current density, showing that the nonlinear conduction is clearly non-thermal. We also note that the temperature changed from 283 to 310 K for 0.03 A/cm^2, when the set temperature was swept from 253 to 313 K. This is not surprising because the measurement was done in an exchange gas of nitrogen to ensure thermally homogeneous environments. As a result, heating/cooling power did not concentrate on the sample, but dissipated around the environment.

Figure 2(b) shows the energy flow IV from the current source calculated from the external current I and the measured voltage drop V. For 0.03 A/cm^2, IV is negligibly small, and the sample is practically in a thermal equilibrium state, where the top-surface temperature should equal the bottom-surface temperature (the temperature at the bottom surface of the sample). With increasing external current density, IV systematically increases, and finally reaches about 50 mW for 15 A/cm^2 (11.6 mA) at 293 K.

Here we discuss to what extent we can predict the sample temperature, and examine the validity of the top-surface temperature measurement. The current flows homogeneously in the bulk, and the Joule heating occurs in the whole sample. In the present setup, the bottom side firmly contacted the heat bath, and the local temperature should be highest around the top surface in a way that the Joule heat inside does not flow to

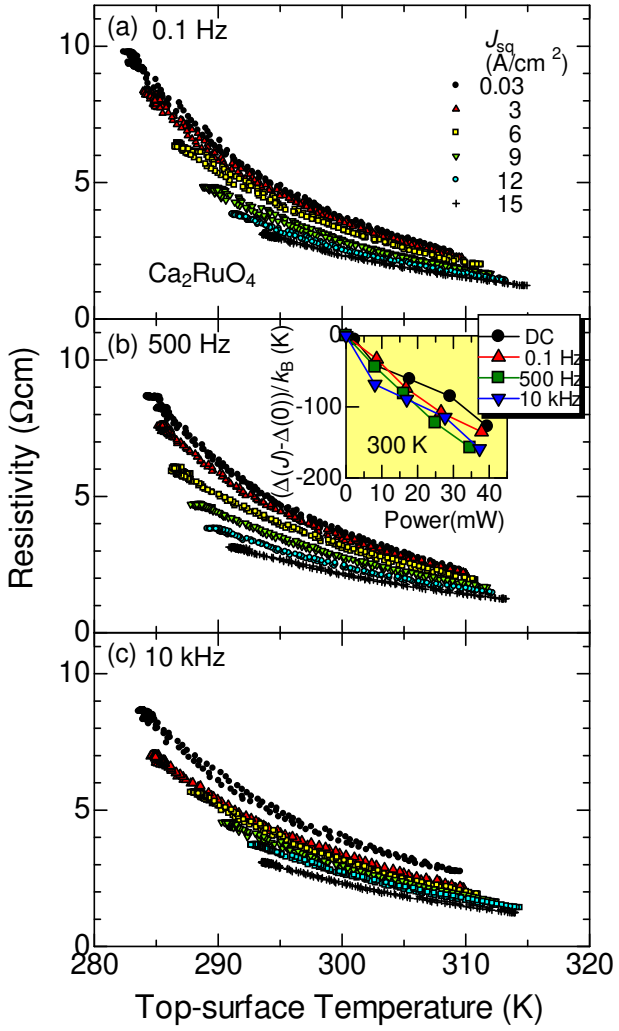

Fig. 3. (Color online) Nonlinear resistivity for ac square-wave current of the single crystal sample of Ca_2RuO_4 plotted as a function of top-surface temperature. (a) 0.1 Hz, (b) 500 Hz and (c) 10 kHz. The inset shows suppression of the Mott gap evaluated from the nonlinear resistivity (see text).

the top surface. Then we can estimate a net heat current along the cross-plane direction in terms of $K_\perp(T_t - T_b)$, where $K_\perp$ is the thermal conductance of the sample along the cross-plane direction. T_t and T_b are the top-surface and bottom-surface temperatures, respectively. Regarding T_b as the temperature for 0.03 A/cm^2 ($T_{0.03}$), we can plot $K_\perp(T_t - T_{0.03})$ in Fig. 2(b). The dotted line represents a cross-plane heat current for the lowest set temperature with $K_\perp$ = 3.7 ±0.2 mW/K. Similarly, the dashed line represents a cross-plane heat current for the highest set temperature with $K_\perp$ = 3.3±0.2 mW/K. Putting the sample dimension of 1.57×0.30×0.26 mm^3, we get a real value of $K_\perp$ to be 3.3±0.5 mW/K from $\kappa_\perp$ = 1.8±0.3 W/mK.

This coincidence implies that most of the Joule heat of $Q \sim IV$ mainly dissipates to the heat bath via conduction, even though actual energy dissipation is much more complicated. The radiation is evaluated to be around 30 μW for T_t = 310 K and T_b = 300 K through the Stephan-Boltzmann law. This is actually found to be negligibly small in comparison with 10 mW, showing that the Joule heat does not flow to the top surface. In this situation, the temperature can be expressed by $T(z) = T_t - \rho j^2 z^2/2\kappa_\perp$ where z is the depth from the top surface based on a one-dimensional model of heat conduction. ρ, j and $\kappa_\perp$ are the resistivity, the current density and the cross-plane thermal conductivity, respectively. This equation indicates that $K_\perp(T_t - T_b) = IV/2$ and differs by a factor of two from $Q = IV$. We cannot explain this difference at present. A finite thermal resistance at the sapphire plate may play an important role, or the one-dimensional model gives an oversimplified picture. Nonetheless we can say that the temperature difference is roughly estimated from IV. The temperature variation will be less than 3 K in the sample for $IV \leq$10 mW, and the sample temperature can be identifed as the temperature for IV = 0 within an uncertainty of ±0.5% at 300 K.

One may suspect that the current does not flow uniformly owing to the temperature difference along the cross-plane direction. In the present sample, the resistivity decreases around 12 % from 300 to 303 K, and thus the current density decreases by 12% from bottom to top for IV = 10 mW. An uncertainty of 12% is of the same order of other experimental constraints such as non-rectangular shape of the sample (Fig. 1(a)). The observed nonlinear conduction is beyond this uncertainty,

Figure 3 shows the ac resistivity measured with square-wave current plotted as a function of the top-surface temperature against various external square-wave current density J_{sq}. As clearly shown, nonlinear conduction is observed for all frequencies, and is essentially independent of frequency. This means that the conduction electrons cannot see the difference between dc and 10-kHz ac current. In other words, a time scale for the nonlinear conduction is shorter than 10^{-4} s in the electron sector. As is widely known, the relaxation time of conduction electrons in conventional metals is of the order of femto to pico seconds,[22] and thus this frequency independence is quite reasonable.

Figure 4 shows the nonlinear resistivity for square-pulse current plotted as a function of top-surface temperature. For a pulse of 12 ms, the nonlinear conduction is clearly seen with increasing the pulse current density J_p, as shown in Fig. 4 (a). On the contrary, the non-linearity is severely suppressed for a pulse of 1 ms, as shown in Fig. 4 (b). We already evaluated the time scale for the conduction electron to be shorter than 10^{-4} s, which is one-order-of magnitude shorter than the pulse width of 1 ms. This indicates that the energy flow does not seem to dominate the nonlinear conduction. The essential difference between the square wave and the square pulse is that the energy dissipation is steady in the former but relaxes in the latter. Thus we conclude that *a necessary condition for the nonlinear conduction in Ca_2RuO_4 is a steady dissipation of energy flow, rather than a steady current flow (or dc electric field) that has been considered as primary for other non-ohmic conductors*.

Let us analyze the nonlinear resistivity in terms of the current-induced Mott gap suppression. We have proposed a phenomenological expression for the resistivity given as

$$\rho(J,T) = \rho_\infty \exp\left(\frac{\Delta(J)}{k_B T}\right), \qquad (1)$$

where $\Delta(J)$ is the current-dependent gap, and ρ_∞ is the resistivity in the high-temperature limit.[12,23] This expression is minimal in that it can cover the temperature and current dependence for a non-ohmic insulator. Accordingly, the ratio of the resistivity $\rho(J)/\rho(0)$ gives the degree of the gap suppres-

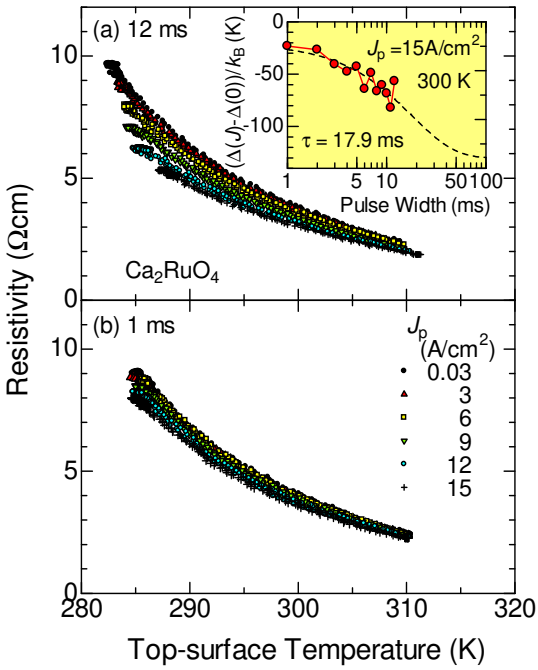

Fig. 4. (Color online) Nonlinear resistivity for square-pulse current of the single crystal sample of Ca_2RuO_4 plotted as a function of top-surface temperature for a pulse width of (a) 12 ms and (b) 1 ms. The inset shows suppression of the Mott gap evaluated from the nonlinear resistivity plotted as a function of pulse width. The dashed curve represents single-exponential fitting (see text).

sion as

$$\Delta(J) - \Delta(0) = k_B T \ln \frac{\rho(J)}{\rho(0)}, \tag{2}$$

where $\rho(0)$ represents the resistivity in the zero current limit.

The inset of Fig. 2shows the degree of gap suppression $\Delta(J)-\Delta(0)$ evaluated by Eq. (2) plotted as a function of energy flow IV. $\Delta(J) - \Delta(0)$ is linear in IV with a slope almost independent of temperature. The inset of Fig. 3 shows the relationship of $\Delta(J)-\Delta(0)$ to IV is also valid for square-wave current. These results strongly suggest that a key parameter of the gap suppression is *not* the current flow but the steady energy flow or the consequent energy dissipation ($IV \sim Q$). It should be emphasized that the linearity is clearly seen below 10 mW, where the temperature can be regarded as homogeneous in the sample. We should also note that this linear relation holds under pressure less than 0.5 GPa (not shown), though the sample temperature was to be precisely evaluated.[24] Together with the results shown in Fig. 4, we conclude that a necessary condition of the nonlinear conduction is a thermally steady state where the energy flow and dissipation are well relaxed.

Finally let us evaluate a time scale for the thermally steady state for the nonlinear conduction of Ca_2RuO_4. The inset of Fig. 4 shows $\Delta(J) - \Delta(0)$ plotted as a function of pulse width. The dotted curve is an exponential fit given by

$$(\Delta(J) - \Delta(0))/k_B = Ae^{-t/\tau} + B, \tag{3}$$

where A = 109 K, B = -130 K and τ = 17.9 ms are fitting constants. The physical meaning of τ is the relaxation time to realize a thermally stable state. If we use the cross-plane thermal conductivity of 1.8 W/mK and the specific heat of 6.9×10^2 J/kgK, we get the thermal conductance $K_\perp$ of 3.3 mW/K and the heat capacity C of 4.5×10^{-4} J/K. Thus the thermal relaxation time is estimated to be $C/K_\perp$ = 140 ms. Although this is one-order of magnitude longer than τ = 18 ms, we regard this estimation satisfactory because this may overestimate C because Joule heating occurs everywhere in the sample, so it may quickly dissipate to the heat bath near the bottom surface.

At present we cannot specify a mechanism why the thermally steady state is necessary for the nonlinear conduction. One possibility is that the nonlinear conduction affects the lattice through the strong electron-lattice coupling, so that the lattice system needs to be relaxed under external current to retain a suppressed value of the Mott gap. Specifically, the external energy flow changes the RuO_6 distortion in Ca_2RuO_4 in order to accept the non-equilibrium Mott gap consistently between the electron and lattice sectors.[16] To do so, the electron and lattice systems feel the same temperature, whereas the electron temperature is much higher than the lattice temperature in high-mobility semiconductors in high electric field. This situation is similar to the nonlinear conduction in the charge-ordered charge-transfer salt θ-(BEDT-TTF)$_2$CsZn(SCN)$_4$, the time scale of which is around 25 ms (40 Hz).[25,26]

In summary, we have carefully measured the nonlinear conduction in the Mott insulator Ca_2RuO_4 against square-wave and square pulse current, and extensively examined the current-induced gap suppression. By putting the thermal conductivity measurements together, we have found that the temperature increase due to the Joule self-heating is quantitatively predicted with a simple heat conduction through the sample to the heat bath. We have further found that the Mott gap suppression scales with the energy flow with a relaxation time of the order of 10 ms. This strongly indicates that a thermally steady state rather than an electronically steady state is necessary for the non-thermal nonlinear conduction in this system. We propose that a strong electron-lattice coupling needs the lattice system to be relaxed in order to retain the current-suppressed non-equilibrium Mott gap.

The authors would like to thank K. Tanabe for an early stage of the present study. They also thank R. Okazaki, Y. Maeno, S. Yonezawa, T. Yoshida, N. Kikugawa, T. Suzuki for close collaboration in Kakenhi Project. This study was supported by a Grant-in-Aid for Scientific Research (Kakenhi Nos. 17H06136, 19H05791). This work was performed under the Cooperative Research Program of " Network Joint Research Center for Materials and Devices " (Nos. 20181015, 20191026, 20201021).

1) Y. Oono and M. Paniconi: Prog. Theo. Phys. Suppl. **130** (1998) 29.
2) S.-i. Sasa and H. Tasaki: J. Stat. Phys. **125** (2006) 125.
3) F. Ritort: *Nonequilibrium Fluctuations in Small Systems: From Physics to Biology* (John Wiley and Sons, Ltd, 2008), Chap. 2, pp. 31–123.
4) N. Garnier and S. Ciliberto: Phys. Rev. E **71** (2005) 060101.
5) V. Y. Pokrovskii, S. G. Zybtsev, and I. G. Gorlova: Phys. Rev. Lett. **98** (2007) 206404.
6) H. Saito, K. Uenishi, N. Miura, C. Tabata, H. Hidaka, T. Yanagisawa, and H. Amitsuka: J. Phys. Soc. Jpn. **87** (2018) 033702.
7) S. Nakatsuji, S. Ikeda, and Y. Maeno: J. Phys. Soc. Jpn. **66** (1997) 1868.
8) C. S. Alexander, G. Cao, V. Dobrosavljevic, S. McCall, J. E. Crow, E. Lochner, and R. P. Guertin: Phys. Rev. B **60** (1999) R8422.
9) M. Braden, G. André, S. Nakatsuji, and Y. Maeno: Phys. Rev. B **58**

(1998) 847.
10) F. Nakamura, T. Goko, M. Ito, T. Fujita, S. Nakatsuji, H. Fukazawa, Y. Maeno, P. Alireza, D. Forsythe, and S. R. Julian: Phys. Rev. B **65** (2002) 220402.
11) P. L. Alireza, F. Nakamura, S. K. Goh, Y. Maeno, S. Nakatsuji, Y. T. C. Ko, M. Sutherland, S. Julian, and G. G. Lonzarich: J. Phys.: Condens. Mat. **22** (2010) 052202.
12) R. Okazaki, Y. Nishina, Y. Yasui, F. Nakamura, T. Suzuki, and I. Terasaki: J. Phys. Soc. Jpn. **82** (2013) 103702.
13) R. Okazaki, Y. Ikemoto, T. Moriwaki, F. Nakamura, T. Suzuki, Y. Yasui, and I. Terasaki: J. Phys. Soc. Jpn. **83** (2014) 084701.
14) Y. Nishina, R. Okazaki, Y. Yasui, F. Nakamura, and I. Terasaki: J. Phys. Soc. Jpn. **86** (2017) 093707.
15) K. Tanabe, H. Taniguchi, F. Nakamura, and I. Terasaki: Appl. Phys. Express **10** (2017) 081801.
16) R. Okazaki, K. Kobayashi, R. Kumai, H. Nakao, Y. Murakami, F. Nakamura, H. Taniguchi, and I. Terasaki: Journal of the Physical Society of Japan **89** (2020) 044710.
17) F. Nakamura, M. Sakaki, Y. Yamanaka, S. Tamaru, T. Suzuki, and Y. Maeno: Sci. Rep. **3** (2013) 2536.
18) S. Nakatsuji and Y. Maeno: J. Solid State Chem. **156** (2001) 26 .
19) I. Hatta, Y. Sasuga, R. Kato, and A. Maesono: Rev. Sci. Instrum. **56** (1985) 1643.
20) T. Baba: Jpn. J. Appl. Phys. **48** (2009) 05EB04.
21) T. Eto, K. Akagi, E. Takashima, T. Noda, T. Suzuki, and F. Nakamura: Extended Abstract for the JPS Meeting **71.2** (2016) 2216.
22) N. W. Ashcroft and N. D. Mermin: *Solid State Physics* (Thomson Learning, 1976).
23) F. Sawano, T. Suko, T. S. Inada, S. Tasaki, I. Terasaki, H. Mori, T. Mori, Y. Nogami, N. Ikeda, M. Watanabe, and Y. Noda: J. Phys. Soc. Jpn. **78** (2009) 024714.
24) K. Toda: Master's Thesis, Nagoya University (2018).
25) F. Sawano, I. Terasaki, H. Mori, T. Mori, M. Watanabe, N. Ikeda, Y. Nogami, and Y. Noda: Nature **437** (2005) 522.
26) T. Suko, I. Terasaki, H. Mori, and T. Mori: Materials **3** (2010) 2027.